Heliyon 9 (2023) e13814

Contents lists available at ScienceDirect

Heliyon

journal homepage: www.cell.com/heliyon

Research article

A novel IEF-DLNN and multi-objective based optimizing control strategy for seawater reverse osmosis desalination plant

Ahmed Alghamdi *

Department of Chemical Engineering Technology, Yanbu Industrial College, Royal Commission Yanbu Colleges & Institutes, P.O. Box 30346, Yanbu Industrial City, 41912, Saudi Arabia

A R T I C L E I N F O

Keywords:
Probability-based dove swarm optimization-proportional integral derivative (PDSO-PID)
Interpolation and exponential based deep learning neural network (IEF-DLNN)
Neural Network (NN)
Fitness
Iteration

A B S T R A C T

Over the past years, Seawater Desalination (SWD) has been enhanced regularly. In this desalination process, numerous technologies are available. The Reverse Osmosis (RO) process, which requires effectual control strategies, is the most commercially-dominant technology. Therefore, for SWD, a novel Interpolation and Exponential Function-centered Deep Learning Neural Network (IEF-DLNN) and multi-objective-based optimizing control system has been proposed in this research methodology. Initially, the input data are gathered; then, to control the desalination process, an optimal control technique has been utilized by employing Probability-centric Dove Swarm Optimization-Proportional Integral Derivative (PDSO-PID). The attributes of permeate are extracted before entering the RO process; after that, by utilizing the IEF-DLNN, the trajectory is predicted. For optimal selection, the extracted attributes are deemed if the trajectory is present, or else to mitigate energy consumption along with cost, the RO Desalination (ROD) is performed. In an experimental evaluation, regarding certain performance metrics, the proposed model's performance is analogized with the prevailing methodologies. The outcomes demonstrated that the proposed system achieved better performance.

1. Introduction

The oceans, which accounts for 97% of the water on earth, are considered to be the major alternative resource owing to the insufficiency of surface as well as underground potable water sources [1]. Nevertheless, for consumption, seawater is not suitable. Hence, a new source of potable water is required to overcome freshwater scarcity; this can be obtained by employing certain SWD methodologies [2]. Seawater desalination, which is a water treatment process, eliminates salt along with other minerals as of seawater; thus, making them useable for human consumption, and industrial along with agricultural usage [3]. (i) Thermal Desalination (TD) model and (ii) Membrane process are the 2 methodologies utilized by the SWD process. Multi-Stage Flash (MSF) desalination and Multiple Effect Evaporation (MEE) are the TD processes [4]; here, in the process of obtaining fresh water, the seawater is heated first to make vapour and it is then transmuted into liquid water again by condensation [5]. Nevertheless, the traditional thermal energy is overpowered by the membrane process like Sea Water RO (SWRO); moreover, it is deployed in over 90% of the newly constructed desalination plants [6].

Owing to its cost-effectiveness as well as lesser energy consumption, SWRO desalination is an extensively espoused desalination technology [1,2,7,8]. Additionally, when analogized to the TD process, SWRO desalination offers higher-quality drinking water [3–5].

* Corresponding author.
E-mail address: alghamdia@rcyci.edu.sa.

https://doi.org/10.1016/j.heliyon.2023.e13814
Received 9 November 2022; Received in revised form 6 February 2023; Accepted 14 February 2023
Available online 17 February 2023

In a desalination system, heat is utilized to evaporate as well as distillate the seawater whereas, in membrane sort, electrical power is used to pump the seawater via the membranes [6,9,10]. The salt is removed by the permeate membrane and fresh water is provided. Nonetheless, higher energy is required by the SWRO to operate; in addition, it requires higher operation costs. Thus, during the desalination process, to get fresh water effectually as of the seawater, the RO plant output should be optimized. With respect to the use of ANNs in the field of desalination, reverse osmosis technology has been done in the existing methods, which includes optimization of SWRO desalination plant operation [11]. To achieve favourable objective functions like the lowest total annualized cost, lowest freshwater production cost, along with lowest energy consumption, the optimization procedure of any industrial process that subsumes the RO process is deemed to be the most projecting tool [7]. Global Optimization (GO), Non-Linear programming (NLP), Successive Linear Programming (SLP), Mixed Integer NLP (MINLP), Sequential Quadratic Programming (SQP), Genetic Algorithm (GA), and Multi-Objective Optimization (MOO) and GA (MOO + GA) are some of the researches being executed to optimize SWRO for single objective or multi objectives [10].

Plasencia et al. [12] developed a methodology to manage operations on a simple SWRO plant. For optimizing the SWRO desalination plant, 2 Machine Learning (ML) algorithms, Decision Trees (DTs) as well as Support Vector Machine (SVM), were utilized. Regarding error metrics, better performance was delivered by the DT algorithm than by the SVM. Nevertheless, the tree might lose data when variables were categorized in multiple categories; thus, the DT algorithm would consume more time to complete the process. Ahmadi et al. [13] recommended a MOO for a multi-effect desalination unit incorporated with a gas turbine plant development. Therefore, to identify the best decision variables, the GA-centric MOO was employed. The outcomes demonstrated that with a motive steam flow rate of 14 kg/s, the Distilled Water (DW) production was 12,294 m^3/day. Even though an increased number of effects ameliorated the DW production rate, the system's total cost rate was high. Taloba [14] presented an Artificial Neural Network (ANN) to optimize the water treatment process as well as the desalination process. The ANN, which predicted the RO desalination process's operation, was utilized in this methodology; in addition, it was wielded to structure the supply water temperature. The outcomes exhibited that the model was cost-effective. Nevertheless, a higher quantity of data was required to train the ANN; moreover, it might not be reliable with low available data. Zhou et al. [15] proffered a model for the operation optimization of the hydroelectrical energy system, which included SWRO desalination. With the third generation of the constrained Non-dominated Sorting GA (NSGA-III), the MOO problem was addressed. The simulation outcomes displayed that for the computation of total cost along with power stability assessment, the presented optimal operation model was highly appropriate. The presented NSGA III algorithm was highly capable of estimating the system's Pareto-optimal operational plans; however, for the MOO, the convergence was low. Leon et al. [16] introduced a model for the optimization of energy efficiency, cost, carbon footprint, along with ecological footprint with RO membranes on SWD plants. In this methodology, RO membranes with higher surface area together with energy recovery systems, which were utilized to recuperate the brine pressure, were employed for the mitigation of energy consumption. By performing experimental analysis on the Canary Island, it was established that in this model, the operational cost was abated and the energy efficiency was augmented. In the Canary Islands, the suggested model performed well. However, when the process is conducted in other zones, the model's efficacy might get changed. Research group of Di Martino [17] established a Neural Network (NN) centered superstructure optimization model meant for the ROD plant. To capture the membrane behaviour precisely, the feed-forward NN with rectified linear units was employed here. After that, to minimize energy consumption, the ANN was transmuted into a mixed-integer linear programming formulation. The model was energy efficient since at most 51% of the monthly overall ROD energy consumption was constituted by the derived energy consumption. Nevertheless, the activation layer did not consider the negative outputs; thus, creating defects in the output. Toth [18] presented a mechanism for the desalination of saline process water resources grounded on the optimization of Multi-Stage Flash (MSF) distillation as well as RO. In this model, the desalination of saline process wastewater was examined with MSF on ChemCAD professional flow sheet simulator; then, it was analogized with the RO on the WAVE simulator. The outcomes demonstrated that the MSF obtained 11.7% whereas it was between 3.0% and 12.6% in the case of RO; thus, suitable for the desalination process. Nevertheless, whilst utilizing the ChemCAD simulator, the process became slow. Karimanzira and Rauschenbach [19] presented a predictive control model aimed at the ROD plant regarding a deep learning model. The Nonlinear Model Predictive Controller (NMPC) was utilized for ROD; here, the Long Short Term Memory (LSTM) was utilized as a predictive model. The outcomes displayed that the system provided a better performance on permeate flow rate. Nevertheless, owing to the usage of LSTM, more storage capacity was required for the presented work. Ehteram and co-workers [20] developed a methodology for the ROD plant's efficiency evaluation regarding hybridized Multi-Layer Perceptron with Particle Swarm Optimization (MLP-PSO). Here, the investigation was done regarding a one-week advance prediction of permeate flow rate for the Sistan as well as Baluchistan provinces. The outcomes demonstrated that in the prediction of permeate flow rate, the present model obtained better performance than the SVM and M5Tree models. However, the system performed slowly owing to the PSO's slow convergence speed. Musharavati et al. [21] presented a MOO of biomass gasification to produce electricity along with desalinated water by utilizing Grey Wolf Optimizer (GWO) as well as ANN. It mitigated the cost and obtained higher energy efficiency. To abate the computation time, the ANN was employed in the optimization process. Here, the total energy computed was 15.61%. Nevertheless, owing to the GWO's lower convergence, the process became slow as time passed.

The prevailing works for the optimization of SWRO desalination have limitations on the efficient production of fresh water. The limitation in existing works is that the controller feed is directly given to the RO plant without considering the unnecessary factors that are not required for the desalination process, which requires more energy consumption. Also, taking all the input data to process, the RO plant requires more cost; hence it cannot be considered as an efficient method. The conversion efficiency of the existing system is also high. By considering these limitations, the aim of the proposed methodology is to develop a better controller strategy and a novel optimization technique to overcome these limitations.

2. Proposed optimal control strategy for sea water reverse osmosis desalination plant

Here, to produce fresh water, a novel IEF-DLNN and multi-objective-based optimizing control system have been proposed for SWD. For input data, an optimal control strategy has been discovered; then, attributes are extracted whilst the trajectory is presented. Furthermore, the optimal control strategy is adopted for the ROD process. Fig. 1 exhibits the proposed scheme's block diagram.

2.1. Input data

Here, seawater conductivity, seawater pH, feed pressure, time, feed flow rate, feed temperature, and feed conductivity are the data gathered for developing the control strategy for the RO plant. After that, the collected information is provided as input into the proposed SWRO desalination plant system. The input data being collected is demonstrated as per the following Eq. (1);

$$D_n = \{D_1, D_2, D_3, \ldots\ldots.D_N\} \tag{1}$$

where, the number of data is specified as D_n.

2.2. Optimal control selection

Here, to control the desalination process, by utilizing the PDSO-PID model, the optimal control selection is deemed for the given input data D_n. In this, the PID controller is utilized; however, in some cases, the whole process's performance might get affected by the controller parameters (that is to say, giving an error); thus, it required optimal parameter selection. For optimal parameter selection, the PDSO algorithm is utilized. Generally, in the search space, the doves search the crumbs; here, some doves might get gratified with the crumbs but not all. To spot more crumbs, the unsatisfied doves fly forward. Slowly, the spots could be occupied by the remaining fed doves with the most crumbs. The Dove Swarm Optimization (DSO) is developed by inspiring such behaviours of the dove. Nevertheless, selecting the learning rate randomly to update the satisfied dove's position might lead the system not to provide the optimal solution in the conventional DSO since an over-selection problem may occur with the uppermost selection whereas a local optimum problem may occur with the lowest selection. So, to figure out the learning rate, the selection probability function is proposed here; thus, addressing the aforementioned issues.

The input data are subjected to the PID controller before selecting the optimal parameters. In accordance with the variation between the desired Set Point (SP) and a gauged Process Variable (PV), the PID controller automatically adjusts a control output. It is computed based on Eq. (2);

$$C_n \in D_n = G_p E(\tau) + G_i \int E(\tau)d\tau + G_p \frac{dE}{d\tau} \tag{2}$$

where, the PID controller's output is specified as C, the proportional gain is signified as G_p, the integral gain is notated as G_i, the error value is symbolized as $E(\tau)$, the change in error value is denoted as dE, and the change in time is indicated as $d\tau$.

Next to this, by utilizing the PDSO-PID, the control variables are optimized in terms of the given input data D_n. Here, the optimized control variables are regarded as the number of doves. In the solution space on a rectangular region, the doves are initialized randomly as,

$$C_n = \{C_1, C_2, C_3, \ldots..C_N\} \tag{3}$$

In Eq. (3), the number of doves is represented as C_n. Next, the position vector is initialized as $\omega_{C_m}{}^{\varsigma}$, the epochs $\varsigma = 0$ and degree of satiety for the dove are represented as $\delta_{C_m}{}^{\varsigma}$.After setting the limit, the multi-objective function (that is to say, maximize desalination plant efficiency, minimize operating cost, and minimize energy consumption) is performed at the epoch as a total number of the

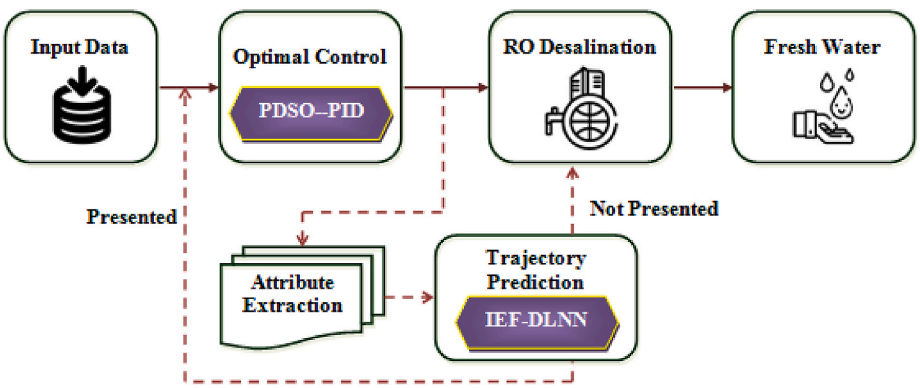

Fig. 1. Block diagram of the proposed methodology.

crumbs in the position of the C_n dove. After that, by utilizing the maximum condition obtained by the fitness function at the epoch $\varsigma = 0$, the dove is located nearby the largest number of crumbs. It is formulated based on the following equation (Eq. (4)).

$$L_{C_n} = \text{argmax}\{\rho(C_i{}^{\varsigma})\} \tag{4}$$

where, the output of the locating dove is represented as L_{C_n}. By utilizing the below equation (Eq. (5)), the satiety degree of each dove $\delta_{C_i}{}^{\varsigma}$ is updated after locating the dove nearest to the crumb.

$$\delta_{C_i}{}^{\varsigma} = \hbar\delta_{C_i}{}^{\varsigma-1} + \varsigma^{(\rho(C_i))} \tag{5}$$

where, the constant is denoted as $\hbar$, and the satiety of the previous epoch of i^{th} dove is signified as $\delta_{C_i}{}^{\varsigma-1}$. After that, by the highest degree of satiety, the most satisfied dove is selected, which is expressed as,

$$C_{sat}{}^{\varsigma} = \arg \max_{1\le i\le N}\{\delta_{C_i}{}^{\varsigma}\} \tag{6}$$

where, the dove is signified as $C_{sat}{}^{\varsigma}$ in the above equation (Eq. (6)), which exhibits the best foraging performance; in addition, it is mocked by other doves in the flock as given in Equation (7).

$$\omega_{C_i}{}^{\varsigma+1} = \omega_{C_i}{}^{\varsigma} + \rho(C_i{}^{\varsigma})\Omega_i{}^{\varsigma}(\omega_{C_{sat}}{}^{\varsigma} - \omega_i{}^{\varsigma}) \tag{7}$$

where, the updating parameter is specified as $\Omega_i{}^{\varsigma}$, and the learning rate to update the dove position vector is depicted as $\rho(C_i{}^{\varsigma})$. Next, by utilizing the selection probability model (Eq. (8)), the learning rate is computed regarding the fitness of every single dove.

$$\rho(C_i{}^{\varsigma}) = \frac{f(C_i)}{\sum_{i=1}^{N} f(C_i)} \tag{8}$$

where, the fitness of an individual *i* in the population is represented as $f(C_i)$, the fitness i^{th} dove is specified as $f(C_i)$, and the fitness of every single dove is symbolized as $f(C_{n(each)})$.Until satisfying the termination conditions, the process is continued by increasing the epochs. Thus, from the controlled variables, the optimal parameters are selected in this manner of selecting the satisfied dove. The output ω_{opt} could be attained at the last epoch of this process and it is represented as an optimal control parameter. The pseudo-code of the proposed PDSO-PID is,

---

Input: collected datainput data D_n
Output: optimal control parameter ω_{opt}
Begin
  Initialize parameters C_n, L_{C_n}, $\delta_{C_i}{}^{\varsigma}$, $\rho(C_i{}^{\varsigma})$, epoch ς
  Random initialization of dove C_n
  Initialize position vector
  Set the epochs ς and degree of satiety for dove $\delta_{C_m}{}^{\varsigma}$
  For $\varsigma = 0$ *to* φ
    While $\varsigma = 0$
      Compute fitness function of each dove
      Locate the dove nearest to the largest number of crumbs
        $L_{C_n} = \text{argmax}\{\rho(C_i{}^{\varsigma})\}$
      Update most satisfied dove
        $C_{sat}{}^{\varsigma} = \arg \max_{1\le i\le N}\{\delta_{C_i}{}^{\varsigma}\}$
      Update position vector of satisfied dove
        $\omega_{C_i}{}^{\varsigma+1} = \omega_{C_i}{}^{\varsigma} + \rho(C_i{}^{\varsigma})\Omega_i{}^{\varsigma}(\omega_{C_{sat}}{}^{\varsigma} - \omega_i{}^{\varsigma})$
    End while
  End for
  Return optimal control parameter
End

2.3. Attributes extraction

The attributes of permeate like dynamic response for permeate flow rate, permeate concentration, and permeate quantity are extracted before implementing the optimal control strategy in the RO phase. To predict the trajectory, informative data about the status of permeate are obtained by performing attribute extraction; subsequently, the attributes being extracted are expressed as,

$$P_n = \{P_1, P_2, P_3, ...P_N\} \ \ (or) \ P_k, k = 1, 2, 3, ...N \tag{9}$$

where, the number of extracted attributes is represented as P_n in Eq. (9).

2.4. Trajectory prediction

Here, the extracted attributes P_n are inputted into the IEF-DLNN, which predicts the trajectory of permeate. DLNN, which is a sort of ML process, utilizes intersected nodes or neurons in a layered structure that looks like the human brain. The input layer, Output Layer (OL), and Hidden Layer (HL) are the 3 layers included. Here, the input layer is the first layer, the OL is the last layer, and HLs are the additional layers of units that lie betwixt the input layer and OL. n-Number of HLs are considered in this methodology. Therefore, providing accurate prediction is always a problem in the NN; in addition, owing to the weight updation procedure, there occur a number of iterations. Moreover, owing to the existence of a number of complex values, the traditional activation function of the sigmoid is not appropriate for this prediction model. To circumvent these issues, in the proposed system, instead of the sigmoid activation function, the exponential activation function is utilized; also, to update the NN's weights, the interpolation methodology is utilized. Fig. 2 illustrates the architecture of IEF-DLNN.

At first, the extracted attributes' outputs are provided to the input layer. Then, from the input layer, the data is given to the HL. Next, for the input attributes, the hidden unit H_k in the HL is computed as,

$$H_k = \beta + \sum_{k=1}^{N} P_k . W \tag{10}$$

In Eq. (10), the bias parameters are represented as β, the k^{th} input attribute is notated as P_k, and the weight parameter obtained utilizing the Interpolation methodology is denoted as W, which is computed using Eq. (11) and is given as,

$$W = b_{1(tarvar)} + \left(a_{tar} - a_{1(tar)}\right) \frac{b_{2(tarvar)} - b_{1(tarvar)}}{a_{2(tar)} - a_{1(tar)}} \tag{11}$$

where, the target and target variation values at one point are symbolized as $a_{1(tar)}$ and $b_{1(tarvar)}$, and the target and target variations at another point are represented as $a_{2(tar)}$ and $b_{2(tarvar)}$. Therefore, the HL's output is fed into the OL. In the OL, the exponential activation function is measured as,

$$\alpha = e^{\aleph(H_k - W)} + \beta \tag{12}$$

where, the output unit is denoted as α, and the radial basis function is specified as $\aleph$. Eventually, the output of Eq. (12) could be classified as the trajectory presented or not presented, which are represented as α_{pre} and α_{not} respectively. For optimal selection, the extracted attributes are considered if the trajectory is present, or else, to mitigate energy consumption along with cost, the ROD is performed.

2.5. RO desalination

Water is taken from the sear after setting all the parameters as well as strategies for the ROD process; then, the first treatment is performed to remove impurities, oil, seaweed, rubbish, et cetera. The saltwater is subjected to RO after removing the organic substances. Following the filtration process, by utilizing a centrifuge, the waste from the pre-treatment is dried, which is either reused or removed for disposal. The freshwater is passed via the demineralization as well as chlorination process; subsequently, it is stored for distribution.

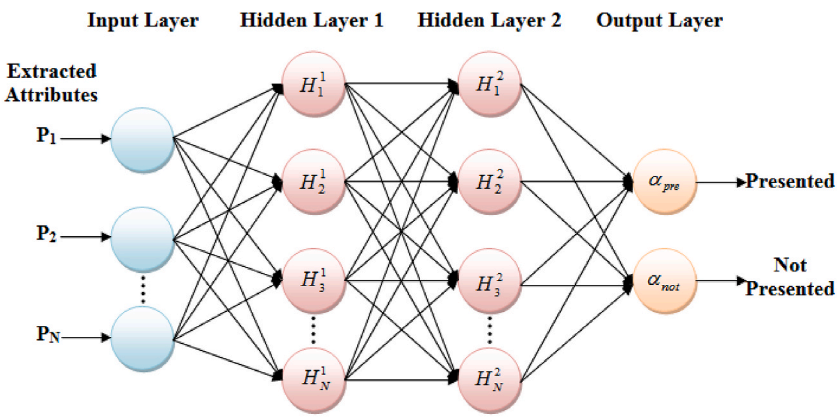

Fig. 2. Structure of proposed IEF-DLNN.

3. Results and discussion

Here, the proposed SWRO desalination is assessed. The proposed system is executed in MATLAB.
Software and system details:

Software: MATLAB (version R2022a)
Processor: Intel core i7
CPU Speed: 3 GHz
OS: Windows 11
RAM: 16 GB

3.1. Performance analysis

Controller and trajectory prediction are the two segments that are performed to assess the proposed model's performance. Additionally, for the analysis of the controller, the fitness vs iteration analysis is also performed.

3.1.1. Performance analysis for the controller

DSO-PID (DSO-PID), Salp Swarm Optimization-PID (SSO-PID), Whale Swarm Optimization-PID (WSO-PID), and PSO-PID are the prevailing methodologies with which the proposed PDSO-PID is analogized regarding conductivity energy along with fitness function.

In Fig. 3, the proposed model's time response analysis is analogized with the prevailing algorithms. The graph shows that the proposed system's conductivity initially starts below 1. For all algorithms, the conductivity increases as the time increases; then, the proposed algorithm's conductivity remains constant after 10 s. Nevertheless, when analogized with the prevailing DSO-PID, SSO-PID, WSO-PID, and PSO-PID algorithms, the proposed one showed better conductivity. Consequently, the proposed algorithm has a better response time.

The proposed model is evaluated regarding the fitness function and is analogized with the conventional models in Table 1. Here, fitness is analyzed to estimate the objective functions' efficiency. For every iteration, the proposed algorithm attained higher fitness. For 50 iterations, the proposed methodology attained a fitness of 96, which is greater than that of the prevailing DSO-PID (91), SSO-PID (87), and PSO-PID (78) models. Similarly, for every iteration, the fitness is computed and correlated with the prevailing models. The overall analysis showed that for the optimal control strategy, the proposed model is highly suitable.

3.1.2. Performance analysis for trajectory projection

Regarding Root Mean Squared Error (RMSE) and accuracy, the proposed IEF-DLNN model is analogized with the conventional DLNN, Convolutional NN (CNN), ANN, together with SVM methodologies.

To detect the prediction errors' deviation, the RMSE is computed. Fig. 4 shows the RMSE analysis of the proposed IEF-DLNN algorithm in contrast to the prevailing DLNN, CNN, ANN, and SVM models. With lower RMSE, the model shows better performance. The proposed technique attained a deviated value of 0.056. However, the prevailing DLNN, CNN, and ANN attained 0.084, 0.102, and 0.116 respectively. Therefore, it is proved that in the output prediction, the prevailing methodologies are dominated by the proposed framework.

In Table 2, the proposed model is analogized with the prevailing DLNN, CNN, ANN, along with SVM methodologies regarding accuracy. Accuracy determines how accurately the system produces the optimal output. The proposed framework attained an accuracy of 96.85%, which is higher than the SVM classifier by 33.84% and higher than the DLNN algorithm by 2.7%. Thus, it is clear that for trajectory prediction, the proposed IEF-DLNN algorithm is more appropriate.

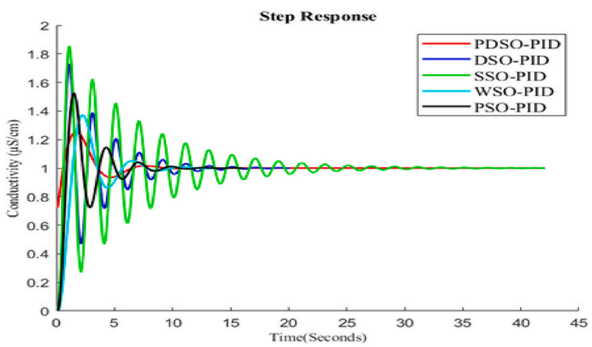

Fig. 3. Conductivity analysis.

Table 1
Fitness vs iteration analysis.

Algorithms	10	20	30	40	50
Proposed PDSO-PID	74	78	86	92	96
DSO-PID	69	73	79	86	91
SSO-PID	64	61	74	82	87
WSO-PID	58	60	68	76	82
PSO-PID	54	59	62	72	78

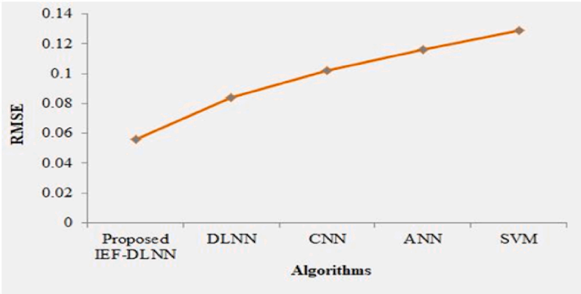

Fig. 4. RMSE analysis for the proposed IEF-DLNN approach.

Table 2
Comparative Analysis of the proposed and prevailing algorithms regarding the accuracy.

Algorithms	Accuracy (%)
Proposed IEF-DLNN	96.85
DLNN	94.23
CNN	86.56
ANN	75.62
SVM	72.36

3.1.3. Performance analysis of permeate flow rate

Here, regarding RMSE, the outcome of permeate flow rate is analyzed. The system attains better efficacy with a lower error rate. The RMSE attained by the proposed model is 0.0079 whereas the prevailing models attained the RMSE in the range of 0.0083–2.322 as given in Table 3. The overall analysis shows that when compared with the prevailing models, the proposed one works more effectively.

Fig. 5 exhibits the graph regarding flux and permeate concentration. Fig. 5(a) displays the alterations in permeate flux at diverse applied pressure with a constant temperature. The outcomes exhibited that an augment in applied pressure generated an augment in the flux. Similarly, Fig. 5(b) shows the concentration of permeates at diverse applied pressure with a constant temperature. From this graph, it is illustrated that the concentration of pressure lessened with an increase in pressure.

The desalination capacity of the proposed model is shown in Fig. 6. A process that takes away mineral components as of saline water is termed desalination. The capacity that is used to calculate desalination is called desalination capacity. At stage 5, the desalination capacity increased to 5.9 L. From the graph, it is concluded that an increase in the desalination stage increases the desalination capacity.

Fig. 7 exhibits the comparative analysis of the proposed model and the existing models regarding energy efficiency. In existing models, such as SVM [12], LSTM [19], and MLP-PSO [20], the models never used trajectory prediction before the desalination process,

Table 3
Comparative Analysis of the proposed and existing algorithms in terms of the permeate flow art.

Authors	permeate flow rate (RMSE)
Proposed research	0.0079
(Marichal Plasencia et al., 2021)	0.0104
(Karimanzira and Rauschenbach, 2020)	0.0083
(Ehteram et al., 2020)	2.322

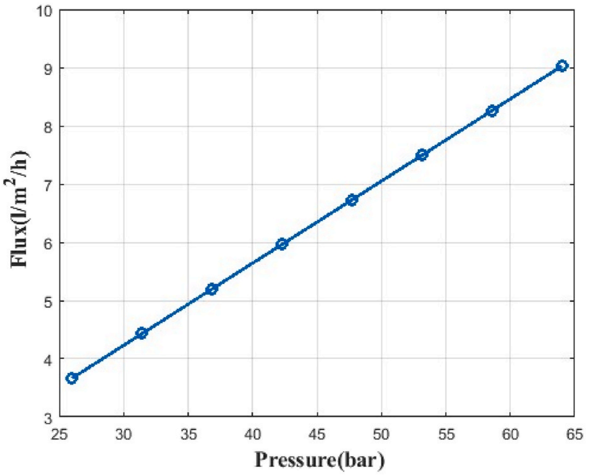

(a)

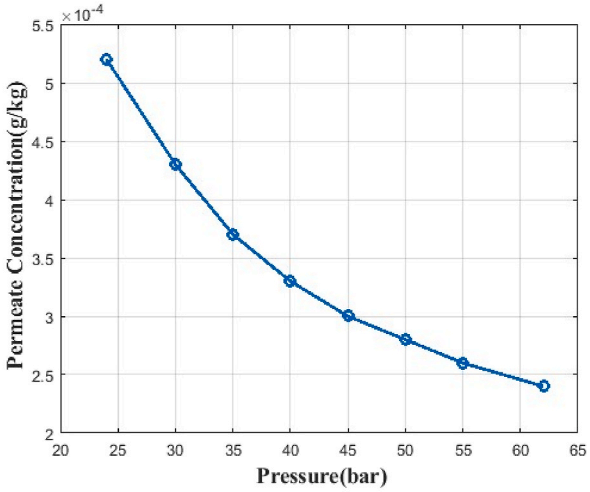

(b)

Fig. 5. Graph in terms of (a) flux and (b) Permeate concentration.

which leads to lower efficiency of the model. But, in the proposed system, the trajectory prediction was carried out before the desalination process, which improves the energy efficiency of the proposed model. Hence, it is concluded that the proposed model is more efficient in seawater reverse osmosis desalination plants.

4. Conclusion

For the SWRO desalination plant, a novel multi-objective optimization control strategy and an IEF-DLNN classifier have been proposed in this research methodology. Here, by utilizing the PDSO-PID model, the optimal control strategy of the SWRO desalination process is performed. After that, by employing the attribute extraction as well as prediction methodology, the trajectory is predicted. In this work, to predict trajectory, the IEF-DLNN is utilized. For the proposed model, experimental evaluation was performed; subsequently, the outcomes obtained were analogized with the prevailing methodologies. Experimental analysis is conducted for the proposed method and is compared with the existing approaches. From the results of all metrics, it is concluded that the proposed model achieved an accuracy of 96.85%, which shows the efficiency of the model. Therefore, the outcomes obtained confirmed that for the SWRO desalination plant, the proposed algorithm shows better performance. To predict the classifier output, the looping of the proposed process consumes a little more time. In the future, to overcome this issue, the attributes will be extracted earlier to mitigate the operational cost further.

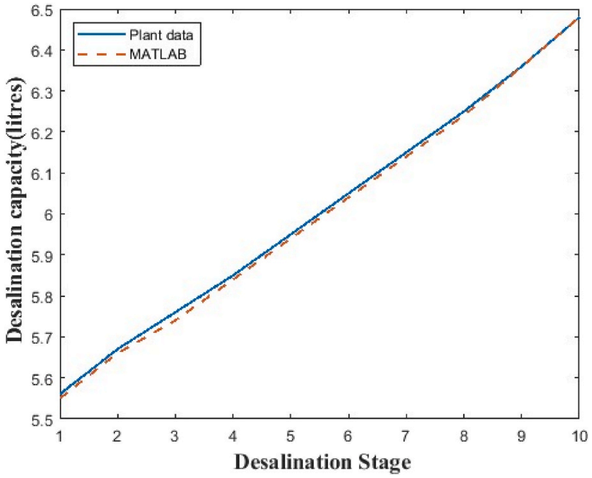

Fig. 6. Desalination capacity of the proposed model.

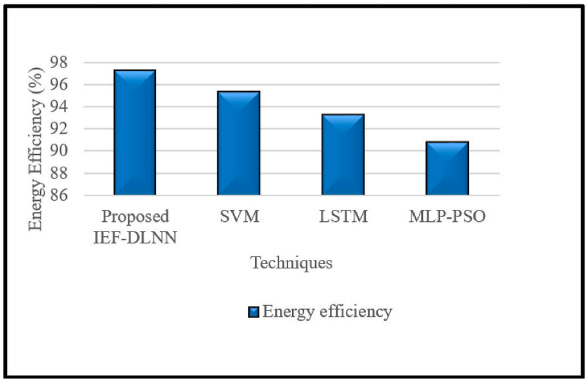

Fig. 7. Comparative analysis of proposed and existing models.

Author contribution

Ahmed Al Ghamdi: Conceived and designed the experiments; Performed the experiments; Analyzed and interpreted the data; Contributed reagents, materials, analysis tools or data; Wrote the paper.

Funding

This research did not receive any specific grant from funding agencies in the public, commercial, or not-for-profit sectors.

Data availability

Data will be made available on request.

Declaration of interest's

The authors declare that they have no known competing financial interests or personal relationships that could have appeared to influence the work reported in this paper.

Abbreviations

IEF-DLNN Interpolation and Exponential Function based Deep Learning Neural Network
PDSO PID Probability-based Dove Swarm Optimization-Proportional Integral Derivative
RO Reverse Osmosis

MSF	Multi-Stage Flash
MEE	Multi-Effect Evaporation
SWRO	Sea Water Reverse Osmosis
NLP	Non-linear programming
GO	Global Optimization
SLP	Successive Linear Programming
SQP	Sequential Quadratic Programming
MINLP	Mixed Integer Nonlinear Programming
GA	Genetic Algorithm
MOO	Multi-Objective Optimization
DT	Decision Trees
SVM	Support Vector Machine
ANN	Artificial Neural Network
NSGA	Non-dominated Sorting Genetic Algorithm
NMPC	Nonlinear Model Predictive Controller
LSTM	Long Short-Term Memory
MLP-PSO	Multi-Layer Perceptron with Particle Swarm Optimization
GWO	Grey Wolf Optimizer
PID	Proportional Integral Derivative
SP	Set Point
PV	Process Variable
DSO	Dove Swarm Optimization
SSO	Salp Swarm Optimization
WSO	Whale Swarm Optimization
CNN	Convolutional Neural Network
RMSE	Root Mean Squared Error

References

[1] M.G. Ahunbay, S.B. Tantekin-Ersolmaz, W.B. Krantz, Energy optimization of a multistage reverse osmosis process for seawater desalination, Desalination 429 (2018) 1–11, https://doi.org/10.1016/j.desal.2017.11.042.

[2] F. Yusefi, M.M. Zahedi, M. Ziyaadini, Evaluation for the optimization of two conceptual 200,000 m3/day capacity RO desalination plant with different intake seawater of Oman Sea and Caspian Sea, Appl. Water Sci. 11 (2) (2021) 1–10, https://doi.org/10.1007/s13201-020-01338-5.

[3] R. Rivas-Perez, J. Sotomayor-Moriano, G. Pérez-Zuñiga, M.E. Soto-Angles, Real-time implementation of an expert model predictive controller in a pilot-scale reverse osmosis plant for brackish and seawater desalination, Appl. Sci. 9 (14) (2019) 1–16, https://doi.org/10.3390/app9142932.

[4] M. Elnour, N. Meskin, K.M. Khan, R. Jain, S. Zaidi, H. Siddiqui, Full-Scale seawater reverse osmosis desalination plant simulator, IFAC-PapersOnLine 53 (2) (2020) 16561–16568, https://doi.org/10.1016/j.ifacol.2020.12.780.

[5] T.M. Mansour, T.M. Ismail, K. Ramzy, M. Abd El-Salam, Energy recovery system in small reverse osmosis desalination plant: experimental and theoretical investigations, Alex. Eng. J. 59 (5) (2020) 3741–3753, https://doi.org/10.1016/j.aej.2020.06.030.

[6] K.H. Chu, J. Lim, S.J. Kim, T.U. Jeong, M.H. Hwang, Determination of optimal design factors and operating conditions in a large-scale seawater reverse osmosis desalination plant, J. Clean. Prod. 244 (2020) 1–35, https://doi.org/10.1016/j.jclepro.2019.118918.

[7] O.M.A. Al-hotmani, M.A. Al-Obaidi, Y.M. John, R. Patel, F. Manenti, I.M. Mujtaba, Minimisation of energy consumption via optimisation of a simple hybrid system of multi effect distillation and permeate reprocessing reverse osmosis processes for seawater desalination, Comput. Chem. Eng. 148 (2021) 1–6, https://doi.org/10.1016/j.compchemeng.2021.107261.

[8] A. Al-Kaabi, H. Al-Sulaiti, T. Al-Ansari, H.R. Mackey, Assessment of water quality variations on pretreatment and environmental impacts of SWRO desalination, Desalination 500 (2021) 1–10, https://doi.org/10.1016/j.desal.2020.114831.

[9] M.A. Al-Obaidi, G. Filippini, F. Manenti, I.M. Mujtaba, Cost evaluation and optimisation of hybrid multi effect distillation and reverse osmosis system for seawater desalination, Desalination 456 (2019) 136–149, https://doi.org/10.1016/j.desal.2019.01.019.

[10] M.A. Al-Obaidi, K.H. Rasn, S.H. Aladwani, M. Kadhom, I.M. Mujtaba, Flexible design and operation of multi-stage reverse osmosis desalination process for producing different grades of water with maintenance and cleaning opportunity, Chem. Eng. Res. Des. 182 (2022) 525–543, https://doi.org/10.1016/j.cherd.2022.04.028.

[11] E. Taheri, M.M. Amin, A. Fatehizadeh, M. Rezakazemi, T.M. Aminabhavi, Artificial intelligence modeling to predict transmembrane pressure in anaerobic membrane bioreactor-sequencing batch reactor during biohydrogen production, J. Environ. Manag. 292 (2021) 1–8, https://doi.org/10.1016/j.jenvman.2021.112759.

[12] G.N. Marichal Plasencia, J. Camacho-Espino, D. Ávila Prats, B. Peñate Suárez, Machine learning models applied to manage the operation of a simple swro desalination plant and its application in marine vessels, Water 13 (18) (2021) 1–15, https://doi.org/10.3390/w13182547.

[13] P. Ahmadi, S. Khanmohammadi, F. Musharavati, M. Afrand, Development, evaluation, and multi-objective optimization of a multi-effect desalination unit integrated with a gas turbine plant, Appl. Therm. Eng. 176 (2020) 1–45, https://doi.org/10.1016/j.applthermaleng.2020.115414.

[14] A.I. Taloba, An artificial neural network mechanism for optimizing the water treatment process and desalination process, Alex. Eng. J. 61 (12) (2022) 9287–9295, https://doi.org/10.1016/j.aej.2022.03.029.

[15] B. Zhou, B. Liu, D. Yang, J. Cao, T. Littler, Multi-objective optimal operation of coastal hydro-electrical energy system with seawater reverse osmosis desalination based on constrained NSGA-III, Energy Convers. Manag. 207 (2020) 1–15, https://doi.org/10.1016/j.enconman.2020.112533.

[16] F. Leon, A. Ramos, S.O. Perez-Baez, Optimization of energy efficiency, operation costs, carbon footprint and ecological footprint with reverse osmosis membranes in seawater desalination plants, Membranes 11 (10) (2021), https://doi.org/10.3390/membranes11100781.

[17] M. Di Martino, S. Avraamidou, E.N. Pistikopoulos, A neural network based superstructure optimization approach to reverse osmosis desalination plants, Membranes 12 (2) (2022) 1–26, https://doi.org/10.3390/membranes12020199.

[18] A.J. Toth, Modelling and optimisation of multi-stage flash distillation and reverse osmosis for desalination of saline process wastewater sources, Membranes 10 (10) (2020) 1–18, https://doi.org/10.3390/membranes10100265.

[19] D. Karimanzira, T. Rauschenbach, Deep learning based model predictive control for a reverse osmosis desalination plant, J. Appl. Math. Phys. 8 (12) (2020) 2713–2731, https://doi.org/10.4236/jamp.2020.812201.
[20] M. Ehteram, S.Q. Salih, Z.M. Yaseen, Efficiency evaluation of reverse osmosis desalination plant using hybridized multilayer perceptron with particle swarm optimization, Environ. Sci. Pollut. Control Ser. 27 (13) (2020) 15278–15291, https://doi.org/10.1007/s11356-020-08023-9.
[21] F. Musharavati, A. Khoshnevisan, S.M. Alirahmi, P. Ahmadi, S. Khanmohammadi, Multi-objective optimization of a biomass gasification to generate electricity and desalinated water using Grey Wolf Optimizer and artificial neural network, Chemosphere 287 (P2) (2022), 131980, https://doi.org/10.1016/j.chemosphere.2021.131980.